Journal of Building Engineering 44 (2021) 102900

Contents lists available at ScienceDirect

Journal of Building Engineering

journal homepage: www.elsevier.com/locate/jobe

The effect of door opening on air-mixing in a positively pressurized room: Implications for operating room air management during the COVID outbreak

Arup Bhattacharya [a], Ali Ghahramani [b], Ehsan Mousavi [a,*]

[a] Department of Construction Science and Management, Clemson University, USA
[b] Department of Building, School of Design Environment, National University of Singapore, Singapore

ARTICLE INFO

Keywords:
Positive pressure
Door opening
Infection control
Operating room
Covid-19

ABSTRACT

The effect of the built environment on the predominant indoor airflow patterns is significant. To protect the healthcare workers at the front line from the outbreak of COVID − 19, it is necessary to understand the transmission dynamics of the virus, which has been shown to depend on indoor airflow patterns. In hospital operating rooms (ORs), design requirements pose a unique challenge as the positive pressure in the OR can facilitate virus spread into adjacent spaces, shall a COVID-positive patient require a surgical procedure. Moreover, the turbulent vortexes from door motions could independently increase the probability of virus escape from the OR to the adjacent corridors. Therefore, to obtain critical knowledge about the alteration of flow fields due to door movement in a positively pressurized room and quantify the air mixing across the door, a series of experiments were conducted in a controlled chamber. The results demonstrate significant impacts of the door opening on the airflow patterns. Increased alterations near the door and vortexes penetrating far into the chamber with multiple doors openings warrant further study of the indoor airflow dynamic under door motion. This experimental study proposes an algorithm to quantify the air exchange due to a standard door opening and quantifies this exfiltration of contaminated air up to 2 air changes per hour, that is 10% of the chamber supply airflow rate. The algorithm to quantify the dissipated air quantity and the analyses of interaction between initial conditions and door openings contribute to the originality of this paper.

1. Introduction

The fast and somewhat uncontrollable spread of SARS-CoV-2 has put forward an unparalleled challenge to the healthcare workers who are at the frontline of this battle. The providers of healthcare services are at a disproportionately high risk of contracting the infection, as they are 29% more likely to get infected [1]. Initially close contact infection through respiratory droplets were thought to be the principal route of COVID-19 transmission. But, Morawska and Cao [2] has shown the airborne transmission to be a significant reason behind the spread by summarizing a wide array of studies [2]. Substantive evidence of the virus being airborne has already been established [3]. The on-field studies inside Wuhan Hospitals in China demonstrated the virus's capability to diffuse indoors and travel up to 10 m airborne [4], which projects additional challenges when patients infected with the novel Coronavirus (SARS-CoV-2) had to undergo a non-deferable surgical intervention [5].

The operating room is a very sophisticated, well-ventilated space, susceptible to contamination spread [6]. These spaces are positively pressurized with respect to adjacent spaces to ensure directional airflow driving the contamination away from the patient to prevent surgical site infection [4,7,8]. However, the isolation condition is of utmost importance when a contagious source is inside the operating room, as the breakdown in isolation condition results in unwanted spread of the infectious agents [9]. Hence, it is important to understand the reasons for the unwanted spread in order to maintain the adequate protection and safety for patients and healthcare professionals. It has been shown in a number of studies that external interventions such as occupant movement and door opening can impact the flow field [10–18]. Literature suggests the number of door openings, depending on the type of surgical procedure [19–21], can range up to 37 to 40 [20,21], peaking during pre-incision phase [20] for obtaining supplies, paperwork, shift change, and communication [20–22]. Door openings are particularly crucial

* Corresponding author.
E-mail addresses: arupb@clemson.edu (A. Bhattacharya), bdgalig@nus.edu.sg (A. Ghahramani), mousavi@clemson.edu (E. Mousavi).

https://doi.org/10.1016/j.jobe.2021.102900
Received 7 December 2020; Received in revised form 19 May 2021; Accepted 15 June 2021
Available online 19 June 2021

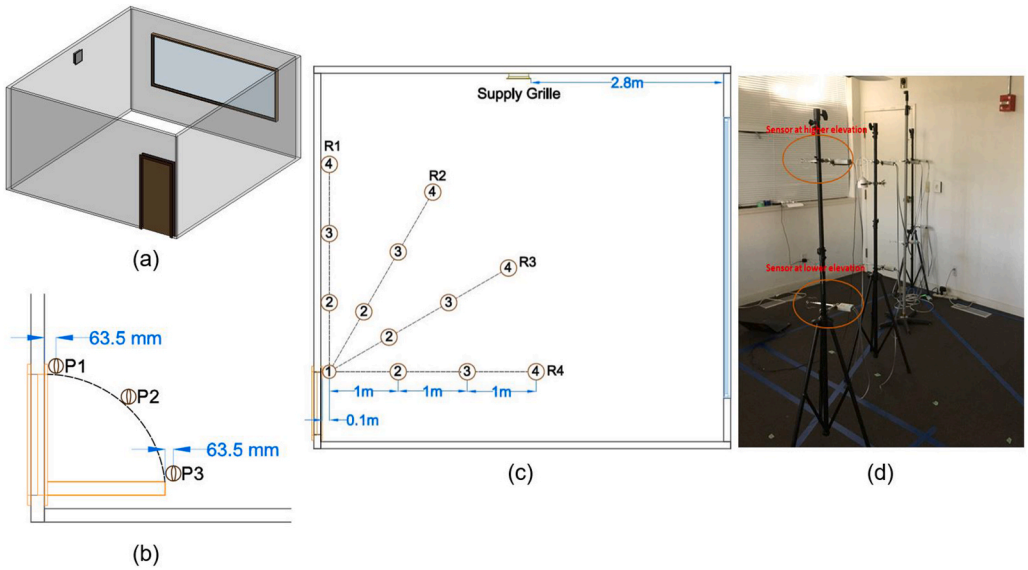

Fig. 1. (a) Chamber geometry – 3D (b) Peripheral Configuration of Sensors (c) Radial Configuration of Sensors (d) Actual Photograph from Test Chamber.

since it disrupts the isolation condition and has the potential to even reverse the differential pressure [9,18,23]. Gustavsson [23] explored the generation of vortices resulting from door opening [23]. Existing studies have concluded that door openings are mass transfer mechanisms through volumetric exchange of air [24–28]. Mousavi et al. (2016) suggested that 5% of the air from a negatively pressurized isolation room can be transported to the cleaner environment, resulting from opening and closing the isolation chamber door [9].

Having established that the door movement has extensive impacts on the existing airflow across two spaces separated with a differential pressure, it is crucial to understand how different human and structural factors impact the air movements. The impacts are different depending on the type of door, opening speed and frequency [19]. For example, it is not clear whether a swing or sliding door results in lower contaminant transport. Lee et al. [29] used computational fluid dynamics (CFD) simulation and conducted experiments to measure inter-zonal volume exchange due to door opening and concluded that under the isothermal condition, there was not much difference between a swinging and a sliding door [29]. On the contrary, Kalliomäki et al. [30] showed that a sliding door could reduce the alterations on the airflow [30]. Mousavi and Grosskopf (2016) demonstrated that the speed of door operation is inversely proportional to exchange volume across the opening through numerical simulation study [9]. Frequent door openings have been associated with increased contamination transfer between spaces [11]. In an experimental study by Hathway et al. [7], it was found that the swept volume due to the swing motion of the door was almost equal to the exchange volume [7].

Apart from air exchange, door motion is also responsible for altering the indoor flow field in a ventilated space. In an experimental study inside an operating room, Zhou et al. [31] demonstrated a difference in flow patterns for the two door movements, as the air flow across the door during the closing period was different than that during opening the door [31]. The generation of vortices at the door tip and propagation of those vortices through the flow field in the room was indicated by Eames et al. [17] in their experiment involving measurements of dye concentrations in a mock-up room [17]. Results showed a significant airflow structure moving along the wall, implying the existence of a separate, near-wall flow field. Mazumder et al. [32] demonstrated higher contaminant concentrations near moving bodies in their simulation of an inpatient ward [32]. This result was further substantiated as both Villafruela et al. [33] and Bhattacharya et al. [18] also demonstrated higher contaminant concentrations associated to traffic movement following a door opening [18,33]. The thermal boundary condition of indoor space is affected by the opening of doors aiding in the generation of lateral airflow movement, specifically found for displacement ventilation [34]. Papakonstantis and colleagues [35] measured the change in flow vectors during door opening and closing using 3-dimensioanl velocity measurements in the proximity of the door [35]. They explained the advection of flow vortex along the wall during opening. In a two-dimensional numerical simulation study of door opening, Bhattacharya and Mousavi [36], showed that the opening and closing movement of the door has profound impacts on the velocity profiles and the direction of streamlines [36]. As demonstrated through that study the flow field recorded higher speed during the closing motion compared to the opening. This could be attributed to velocity residuals due to the opening phase.

In summary, the focus of existing literature has been on understanding the impact of door opening in the volumetric exchange and air mixing. There has been a dearth of pertinent research on characterizing the air mixing with respect to pressure differential and different types of door opening exercise from actual field data. In this study, experiments were carried out in a controlled environment with capabilities to obtain positive pressure levels sufficient to emulate/exceed operating room conditions. The volumetric air exchange has been characterized and quantified under three different pressure differentials across a swinging door for both a single and two-consequent door openings. Several previous studies have investigated the volumetric exchange between spaces separated by a door, ensuring differential pressures at the two compartments from numerical simulation approach [9,29] and experimental approach [23,30]. The novelty of this paper lies in the way it analyzed and quantified potential contaminant migration outside the operating room from door opening, considering the room is positively pressurized. Although some existing studies have looked in to the changes in the velocity field due to door opening [17,31,34,35], changes in the existing flow field due to perturbation induced through door opening and closing motions, and the resultant mixing of supposedly contaminated air containing virulent strains from the patient, with the supplied air inside the chamber, are holistically analyzed in this work. A novel approach to calculate mass flow rate across a door from the measured flow velocity and time of door operation has been proposed. This work is also unique in the way of analyzing the flow characteristics near the door swing periphery and the indoor mixing of contaminated exhaust air under ventilation, due to disruptions in the principal flow direction from door operation.

2. Methodology

2.1. Chamber geometry

A 5.48 m x 5.44 m x 2.5 m experimental facility at the Center for Built Environment in the University of California, Berkeley, with a swing door of dimension 1.98 m x 0.98 m at one corner, was used to conduct the experiments. This sealed facility was equipped to supply air at different flow rate through overhead diffuser, wall mounted grille or through several floor mounted baffles. The 0.3 m x 0.3 m wall-mounted diffuser at a height of 0.3 m from the ceiling, was used for our experiments due to the ease of flow variation through user control (Fig. 1). The supply flow rate created a positive pressure in the room and the excess air left the room through the gaps around the door frame.

2.2. Experimental setup

To observe the patterns and characteristics of indoor airflow and to quantify the volumetric air exchange, emerging from two consequent door opening and closing motions, a series of tests were conducted. To capture the flow characteristics of an indoor space of size 5.48 m x 5.44 m x 2.5 m, at least 16 pairs of omnidirectional sensors would suffice to cover the whole space. Instead, we had 4 pairs. With the limited availability of air velocity measuring instruments, the experiments were conducted in several stages. Therefore, a set of sensing instruments were deployed to obtain near-boundary data at the proximity of the door movement periphery (Fig. 1b) 63.5 mm away from the door tip, there were 3 locations housing the measuring instrument for 8 rounds of tests. The sensing station $P1$ was closest to the door tip when fully closed and when fully opened, the closest station was $P3$, with $P2$ exactly in the middle. At locations $P1$ and $P2$, three sensors were mounted at equal distances to each other, each covering a third of the door height, with the bottom one being 0.66 m above the floor level. Only the bottom two sensors were mounted at location $P3$, owing to the limited number of available sensors.

Another set of 8 unidirectional sensors were arranged in 4 imaginary rows, designated as $R1$ through $R4$, going inside the chamber in a radial direction (Fig. 1c), at two elevation levels. The row $R1$ was parallel to the closed door, and the sensors were at a distance of 0.1 m from the wall, whereas the row $R4$ was perpendicular to the closed door, with rows $R2$ and $R3$ making 30° and 60° angle with $R1$, respectively. The measuring instruments were mounted on tripods along each row in four locations, identified using sensor ids 1 through 4. The first sensing system was the closest to the door tip at a distance of 0.1 m, and the subsequent instruments were located in 1.0 m increments. Moreover, the measuring instruments at the lower elevation were 0.66 m above the floor level, which was a third of the total door height. The higher-level sensors were placed at another 0.66 m from those at the lower elevation, covering two-thirds of the door height from the ground. The denotation of sensors was such that they were identified based on their elevation and location on a row. For example, the second sensor at the lower level (L) of row 3 is identified as $RL32$, or the third senor at the upper elevation (U) of the first row will be identified as $RU13$.

As mentioned previously, the test setups and the perceived analysis from the collected data were focused on understanding the three-dimensional flow fields generated from the swing door movement. The tiered arrangement of sensors provided the possible understanding at two (for radial arrangements) and three (for peripheral arrangement) levels. With the distance between the measuring stations, we were able to follow the evolution of the flow originated from the door opening at least until the middle of the room, given the limited number of sensors and restricted access to the test chamber.

2.3. Door-opening exercises and initial conditions

Different sets of experiments were defined for two different door movements and three initial conditions, provided by the amount of air inlet from the diffuser. For each experiment setup, the experiments were conducted in sets, due to limited access to multiple sensors simultaneously, as expressed in the Experiment Setup section. The two movements of the swing door that opened into the chamber, are defined as follows:

1. Opening and closing the door once in a way that the door opens in the first second of every trial that takes 2 s to complete and stays open for a second before the closing movement completes by another 2 s, i.e., a total opening cycle of 5 s. This represents a typical door opening by a healthcare professional.
2. Opening and closing the door twice with the first cycle finished by second 5, then the door is kept shut for 2 s before replicating the first cycle, i.e. opening through 2 s, keeping ajar for 1 s and closing for 2 s. This scenario could represent a case of quick supply run to the operating room with two immediate door operations.

During both of these settings, each trial of experiments was run for a duration of 60 s while each test was repeated 60 times to ensure statistical consistency. For every set of experiment, the door opening was initiated at the first second, and it was closed at the end of ~ 5s (for opening once) or ~ 12s (for opening twice). The sensors started recording air velocity from the start of door opening at second 1 and continued for a minute. The door was again opened at the first second of the next minute, and these repetitions continued for 60 min. With the absence of any automatic door controlling device, the opening and closing, as well as the timekeeping was done manually. Owing to this reason, the time required for the first cycle to complete was not exactly 5 s and for double operation, not 12 s. The associated deviations for all 60 repetitions of each test based on door operation and initial conditions, are tabulated in Table 1.

Table 1
Experiment conditions.

	Inlet Airflow	Door Opening Exercise	Average Door Operation Time (s)	Data Logging Duration	No. of Repetitions
Test 1	Still	Once	5.38 (σ = 0.21)	60 s	60
Test 2	Still	Twice	12.33 (σ = 1.14)	60 s	60
Test 3	70% Air	Once	5.52 (σ = 0.82)	60 s	60
Test 4	70% Air	Twice	12.49 (σ = 0.24)	60 s	60
Test 5	100% Air	Once	5.42 (σ = 0.39)	60 s	60
Test 6	100% Air	Twice	12.48 (σ = 0.19)	60 s	60

Three different flow regimes were identified, according to the volumetric air flow through the diffuser, which are described below.

- Still air – With the absence of airflow, as the fan and the air handling unit (AHU) responsible for air supply to the chamber were not operating, the initial steady state condition inside the experiment chamber under this scenario was quiescent, and the supply diffuser was shut off.
- 70% fan – The supply fan and the AHU were throttled to operate at 70% of the full capacity. With the exfiltration through the gaps around the door frame, the manometer reading indicated a positive pressure differential of 10 Pa between the room and outside after steady state condition was reached inside the chamber.
- 100% fan – During this flow regime, the supply fan and AHU operated in full capacity. With 190 cfm (90 L/s) [37] air inlet, the steady state reading of the positive differential pressure between the chamber and outside was measured to be 20 Pa.

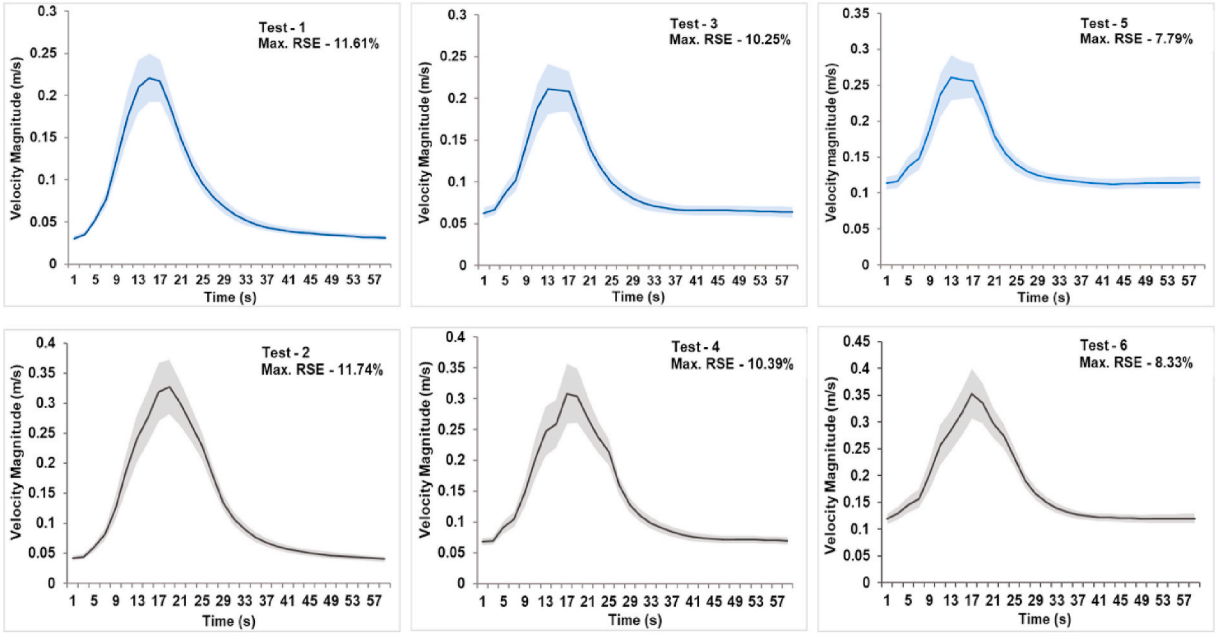

Fig. 2. Data consistency.

2.4. Measurements

Two different types of sensors were used for the experiments. The omnidirectional sensors recorded only the velocity magnitude, whereas the ultrasound sensors logged the components of velocity in three Cartesian coordinates, where the x-axis was along the tangent of the arc made during door opening, y-axis was along the radial of that arc, and z-axis was along the normal to the floor plane. The omnidirectional sensing system is a hot-wire anemometer type velocity measurement transducer known as AirDistSys 5000, manufactured by Sensor Electronic, Poland. The main components included a transducer, a converter and a transmitter. SensoAnemo5100LSF is a transducer with omnidirectional (spherical) sensor with a diameter of 2 mm, measurement speed range of 0.05–5 m/s, 0.02 m/s or 1.5% of reading accuracy of measurement, directional sensitivity error for $v > 2$ m/s of 2.5% the actual value. These omnidirectional anemometers have been previously used in a number of studies to measure air velocity [38–42]. With a maximum logging frequency of one data point every 2 s, these anemometers are designed for low-velocity indoor airflow measurement and are equipped with wide range of frequency response and high sensitivity.

The ultrasound sensing system was lightweight, portable and suitable for indoor airflow measurements, indigenously developed in UC Berkeley's Center for the Built Environment. Employing a new micro-electromechanical systems technology for ultrasonic range-finding, this sensor uses CH-101 ultrasonic transceivers and tetrahedral arrangement of four such transceivers was used that provided enhanced measurement redundancy while measuring 3D velocity components. The anemometer has a resolution and starting threshold of 0.01 m/s, an absolute air speed error of 0.05 m/s at a given orientation with minimal filtering, 3.1° angle and 0.11 m/s velocity errors over 360° azimuthal rotation, and 3.5° angle and 0.07 m/s velocity errors over 135° vertical declination. For more details, please refer these papers [43–46].

The goal of this study was to analyze the air movement originated from opening and closing a swing door to a positively pressurized

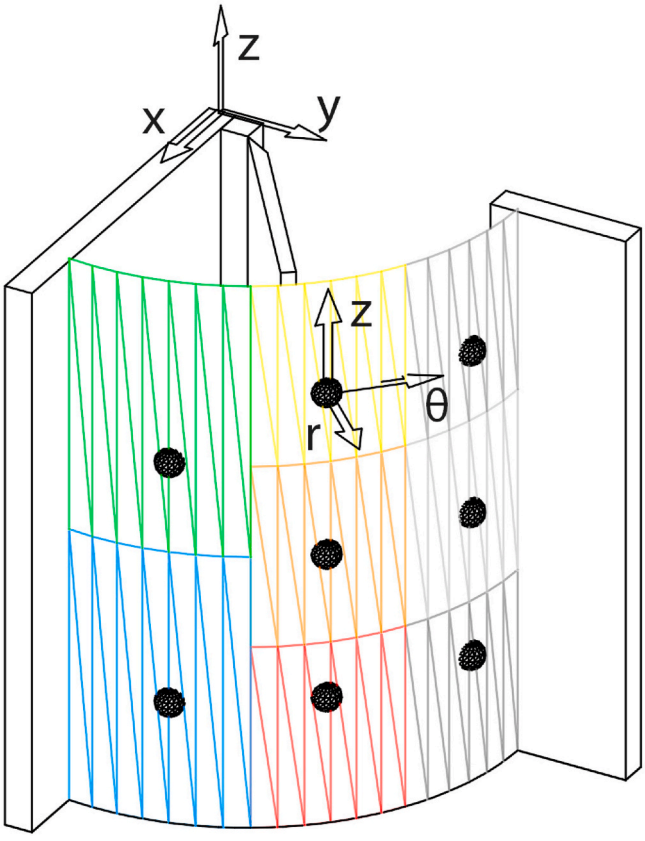

Fig. 3. Placement of sensors and coordinate definitions.

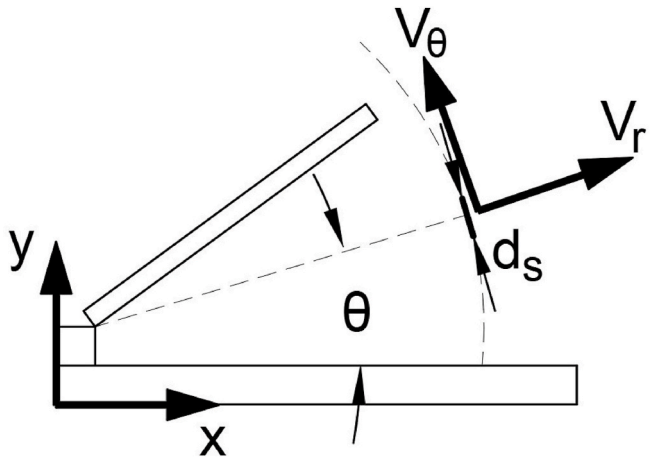

Fig. 4. Cartesian and cylindrical coordinates conversion.

chamber. Since fluctuations in temperatures can generate buoyancy driven airflow, it was important to measure such fluctuations in the air temperature inside the chamber. The omnidirectional sensors recorded temperature along with the velocity values. The average temperature across all experiments was 23.7 degree Celsius, with a standard deviation of 0.025, which was negligible in terms of generating buoyant flows and an isothermal condition inside the chamber could be assumed.

2.5. Statistical analysis

As explained earlier, the sensing instruments recorded time-averaged values of velocity magnitudes for 60 s in each experiment, which was repeated 60 times. Those data points were averaged to obtain temporal trends and transient velocity profiles. The collected data demonstrated consistency at each point in time. The consistency was assessed by relative standard error (RSE), defined as percentage of data standard error over the mean velocity. Depicted in Fig. 2, the solid lines portray the mean velocity for each set of experiment and the surrounding shaded region displays the standard error bounds. It is noteworthy that the maximum distance between the bounds are associated to the time of door movement cycle, probably due to the stochastic patterns in the turbulent flow.

2.6. Mass transport calculations

Placement of sensors brought about the opportunity to calculate air-mixture at the door due to door opening for various pressurization scenarios. The ultrasound sensors placed immediately around the opening radius of the door were used to measure the three dimensional velocity of air around the door. The results of velocity measurements by the ultrasound sensors were reported in the global Cartesian coordinates shown in Fig. 3. A conversion of these values to a cylindrical coordinate was convenient in order to measure the mass flow of air through the radius of opening. Formally, the rate of mass transfer on the door swing surface (let's denote this surface by **S** throughout the paper) is $\dot{m} = \frac{dm}{dt}$. Assuming a constant density of air in ambient temperature, we have:

$$\dot{m} = \frac{dm}{dt} = \rho \frac{dV}{dt} = \rho \frac{ds\, dr\, dz}{dt} \tag{1}$$

It must be noted that the tangential (ds) and vertical (dz) differential elements do not change with time where the change of the radial term (dr) with time is velocity v_r. Therefore, Equation (1) will take the following form.

$$\dot{m} = \oint_S \rho v_r\, ds\, dz \tag{2}$$

Knowing that $ds = Rd\theta$ where R is the radius of the door, one can write v_r based on its v_x and v_y components, which is what was measured by the ultrasound sensors(Fig. 4). Thus Equation (2) will turn to:

$$\dot{m} = \oint_S \rho\, R(v_x \cos\theta + v_y \sin\theta)\, d\theta\, dz \tag{3}$$

Ideally, the radial component of velocity (v_r) varies as function of θ and z, and the integral in Equation (3) can be numerically calculated to find the rate of mass transfer through **S**. In our test setting however, we only had measurements of air velocity in eight fixed points. Thus to solve Equation (3) we assumed that velocities measured by each sensor embodied the region around it, as demonstrated by Fig. 3.

The ultrasound sensors collected 6 data points per second, that is 12

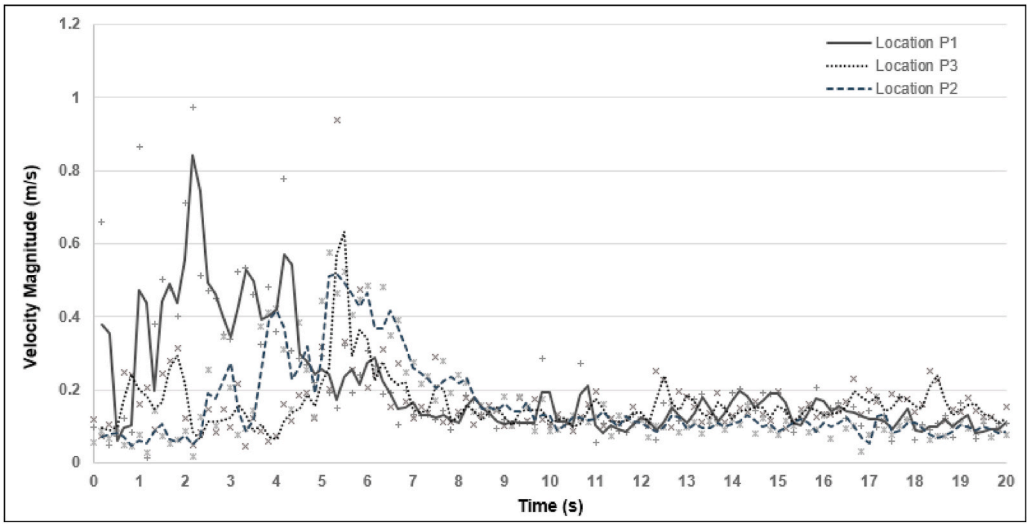

Fig. 5. Transient pattern of air speed from door opening and closing once (test 1).

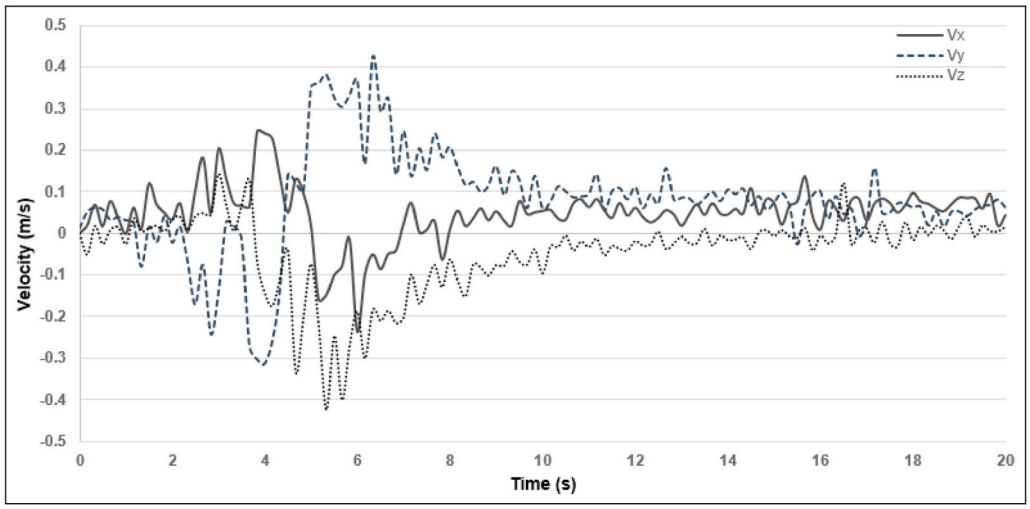

(a)

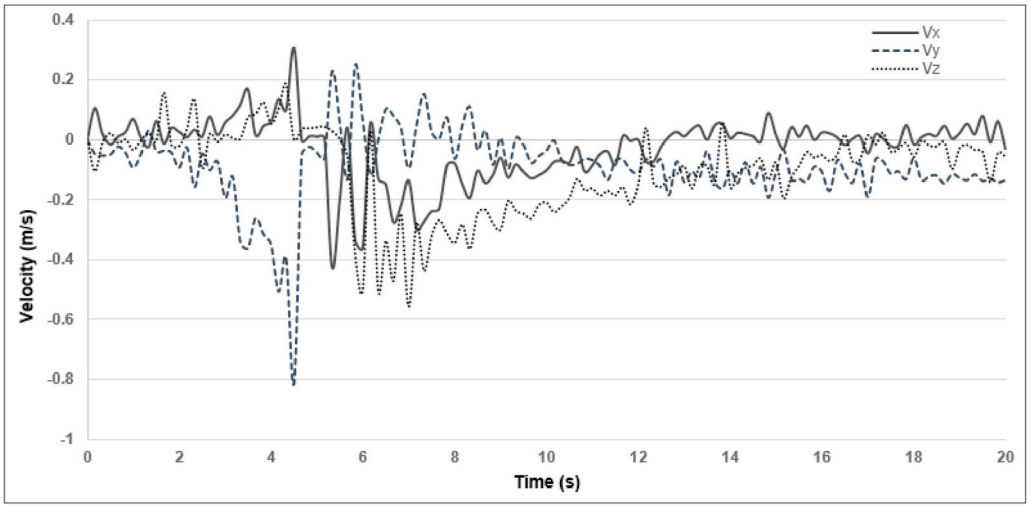

(b)

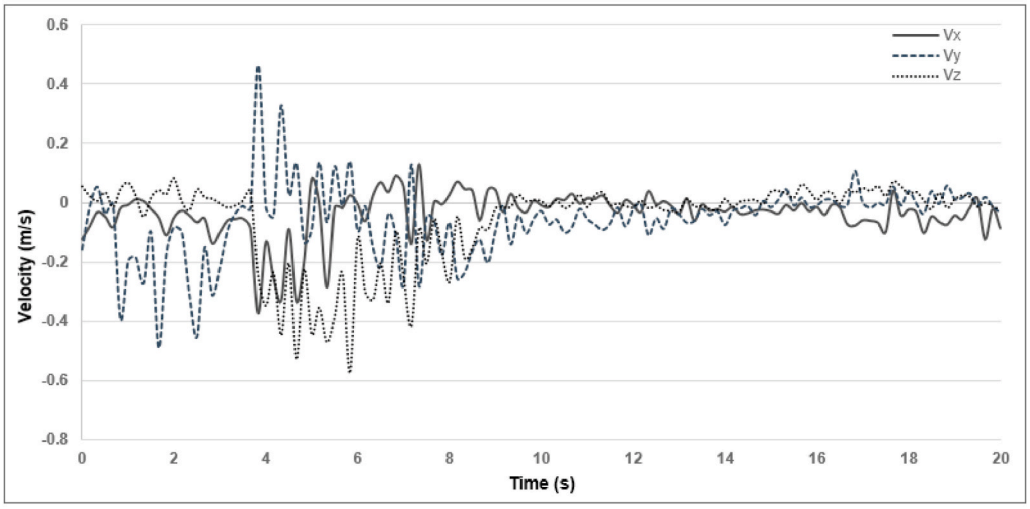

(c)

Fig. 6. Cartesian Components of velocity at location P2 for (a) Test 1, (b) Test 3, and (c) Test 5.

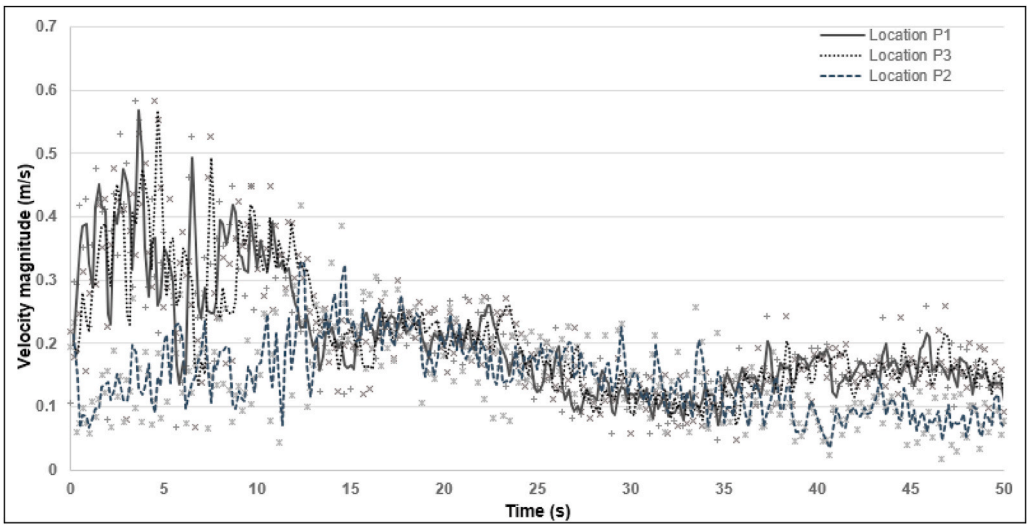

Fig. 7. Transient pattern of Air Speed from Door Opening and Closing Twice (Test 4).

data points from a fully-closed to a fully-open status, a total of 30 data points for a full door opening cycle (i.e., 5 s). To match this, **S** was discretized into 12 vertical sections, each covered three different measurements from the vertically aligned sensors. Further, the opening degree of the door(θ) is also a function of time and it dictates the angular width of **S**, i.e., the space that is exposed to the outside. Algorithm 1 was used to calculate $\dot{m}$. Note that both T_i and v_r are functions of time, and v_r for each piece was embodied by the sensor measurements within its region. One can also take the integral of $\dot{m}$ with respect to time to obtain the amount of air mixture across the door. Based on the coordinate convention and consistent with the positive direction of v_r, negative mass flow means air leaving the room and positive mass flow means air entering the room.

Algorithm 1. Rate of Mass Transfer

Algorithm 1 Rate of Mass Transfer

Let **S** be discretized into n equal vertical pieces of $< s_1, \ldots, s_n >$ and a full door opening cycle take $N = 30$ timesteps (i.e., 5s).
for $t = 1, 2, \ldots, N$ **do**
  define $T_{1\times n}$ vector (initially zero) to determine the exposure of each piece to the outside
  if $t < 12$ **then**
    $T(1:t) = 1$:opening cycle
  else if $t < 18$ **then**
    $T(1:end) = 1$:hold-open cycle
  else
    $T(1:t-18) = 1$:closing cycle
  end if
end for
$\dot{m} = \sum_{i=1}^{n} T_i \cdot v_r$

3. Results and discussion

3.1. Transient flow patterns

The temporal patterns of air movement at the sensing stations near the door swing periphery were analyzed using the Cartesian velocity components, obtained from the ultrasound sensors. These sensors reported 6 data points of velocity components per second at every location.

3.1.1. Door opening once

During Test 1, when the existing initial condition was quiescent air, and there was no other movement than the door movement, changes in three-dimensional air velocities were recorded. The transient pattern is depicted in Fig. 5. At the onset of door opening motion, the sensing station at *P*1 recorded an increase in air speed with a one-second lag. The highest magnitude was recorded at 2.1 s, as the air with high magnitude of velocity followed the moving door. Sensing station at *P*2 began logging an increase in air speed from second 3.5, reaching max during opening at second 4.5 and again peaked during closing at second 5.3. It is noteworthy that the magnitude was higher during closing compared to opening motion. During the opening motion, the initial condition is still air. But while closing, the air in the chamber had a presupposed motion resulting from door opening. Closing the door created a motion, reversing the direction of the previous one, probably affecting the change in velocity. At location *P*3, there is an initial surge, possibly due to the impetus exerted by the door opening that carried the previously stagnant air quickly to the wall. During closing, the moving door is extracting the air inside the chamber, and the wakes following the closing door were recorded at location P3, which showed a peak quickly after closing motion was complete. Fig. 5 demonstrates these changes in velocity magnitude plotted against time.

Even though the magnitude of air had significant patterns that correspond to the door opening and closing duration, the velocity components obtained from the ultrasound sensors led to a deep analysis of door movement. At the beginning of door opening, the moving door

was pushing the still air inside the chamber, which was recorded as a surge in velocity in the positive x-direction (as shown in Fig. 3) and for a small duration, a negative y-component (normal to the door opening direction at $t = 0$ s) of the velocity was detected in location $P1$. As the door continued to open, air wakes were carried with the door, and the y-component of velocity was recorded as negative at point $P2$, as at this point the principal direction of air movement was opposite to the defined y-axis. Moreover, the x-components of velocity was flowing towards the inside of the chamber, i.e., positive x-axis. At location $P3$, when the door was completely open, the generated wakes were being carried by the swinging door, the y-component of velocity was found to be in the negative direction and as the door started closing, this component became positive. At the end of door opening, the moving air came across and moved along the wall perpendicular to the closed door, and a surge of velocity in the positive x direction was recorded. While closing, the door dragged the moving air back with the wakes generated, principally at the direction of negative x-axis and positive y-axis, as recorded in measuring units located at both $P3$ and $P2$. This change in the direction of x-component and y-component while opening and closing is distinctly identifiable in Fig. 6 The increase in velocity components was prevalent until second 15. After the door was fully closed, all components of velocity became stable and near zero, as the air near the door became motionless while the flow field approached steady state given the absence of any further disturbance.

During Tests 3 and 5, air was being supplied in the room, creating a positive pressure inside the chamber. With the supply fans operating, as soon as the door opened, air started moving outside, captured as an increase in negative x-velocity at location $P1$. But the movement of the door, opening against a large differential pressure, displaced a large amount of air, which was captured by the increase in velocity components in the positive y direction at this point in space. The existing air inside the chamber was being pushed during the opening movement, being recorded as positive in the x-direction and negative y-component at the middle of the door movement curve. With continued opening motion of the door, there was more space for the positive pressure to push the air out of the chamber, resulting in the increase in negative x-component of the air velocity. Analogous to the test cases with still air, at the end of the opening motion, the wakes generated was pushed inside the chamber, surging the positive x-component and negative y-component at the end of opening cycle, at location $P3$. But due to the positive pressure, coupled with the closing movement of the door, the prevalent air movement due to the opening motion was reversed quickly. Even though the results obtained with fan operating at 70% and in full capacity were similar, higher quantities of supply air (i.e., higher pressure differentials) resulted in comparatively less significant changes in the flow fields inside the chamber due to the door movement. Lower magnitudes of velocity was observed, and the x-component of velocity was consistently negative, implying almost no air entering the room under this condition (Fig. 6).

3.1.2. Door opening twice

The experiments that consisted of two consecutive opening and closing cycle, the first cycle of door opening, and closing was analogous to those of the experiments involving single door opening and closing. For the test with no ventilation (Test 2), the sensor at location P1 recorded the increase in velocity instantaneously, peaking at close to 3 s for the first time opening. Instruments at location $P2$ also recorded the surge for opening and then a higher magnitude during closing at around 3.5 s and 5.3 s, respectively, for the first round of door operation. But, during the second cycle of door opening – closing, the speed recorded

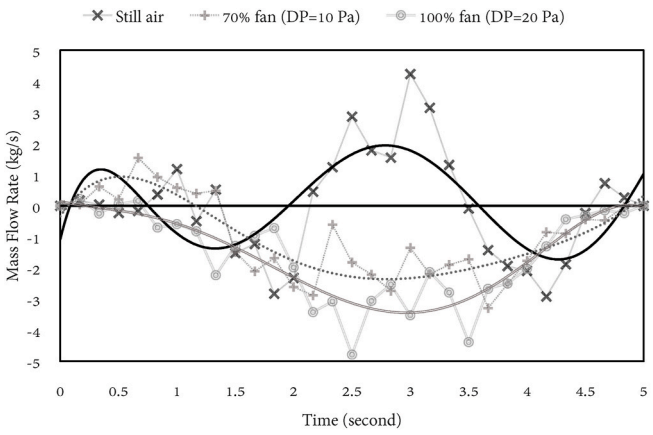

Fig. 8. Mass flow rates in kg/s during door opening for various test conditions.

was higher compared to the first cycle, owing to reasons attributable to the interaction of the repeated motion with the residual movement from the first cycle. Fig. 7 shows the immediate rise in air velocity, recorded by the measuring device in location $P1$, followed by $P2$ and $P3$. The closing motion that followed the door opening, and then another set of consecutive opening and closing for the second cycle stirred the stagnant air, that resulted in higher velocities. The surge in velocity magnitude for the second time door operation was apparent visible for both Tests 4 and 6, as depicted in Fig. 7 for Test 4. Interestingly, significant changes in velocity magnitude was recorded up to 10 s for Test 2, and 15 s for Test 4 and 6 after the door movement was stopped.The 3-dimensional velocity component data, obtained using the ultrasound sensors, revealed more details regarding changes in air flow patterns when two swing door opening occurred consecutively. The data demonstrated similar behavior of air flow patterns during the second cycle of door operation, when compared to the first cycle, with different magnitudes.

During tests with door-opening twice, i.e. Tests 2, 4 and 6, further changes along the time in the transient trends were detected than what was captured during Tests 1, 3, and 5. For the experiments with ventilation on, at the onset of second door opening, the negative v_x from the residual motion is quickly reversed, owing to the directional flow gushing out through the open door. The existing motion of v_y was also reversed for a short while as the swing of the door dragged the air flow opposite to the existing residual flow from the previous closing. During closing, flow along the wall perpendicular to the closed door, was recorded as a positive surge in the x-component and the flow wakes carried by the closing door was responsible for the positive y-components. After the door was closed, the leaking air through the gaps of the door was able to maintain a negative V_x with a magnitude $\sim$ 0.2 m/s.

3.2. Mass flow

As discussed earlier, the opening of door had significant effects on air mixing across the door. In the absence of pressure differentials across the door, air mixing took place both ways. Initially, air entered the room following the inward door swing ($<$ 1.0s). Immediately after, the room air made up for the temporary vacuum created by the large boundary movement by leaving the room and creating vertices at the tip of the door ($\sim$ 1.5s). Then air from the outside began to entrain into the room until the closing cycle started ($\sim$ 3.5s). Then the closing door pushed air out of the room ($\sim$ 3.5 – 5.0s) (Fig. 8). Air velocities inside the room approached background values nearly 10s after the door was completely

Table 2
Total amount of air exchange (kg) across the door for different pressure differentials and door openings.

Door opening Case	Still Air (ΔP = 0 Pa))			70% fan (ΔP = 10 Pa)			100% fan (ΔP = 20 Pa))		
	entering air	exiting air	net	entering air	exiting air	net	entering air	exiting air	net
Opening once	3.38	−2.82	0.56	2.5	−7.53	−5.03	0.00	−7.58	−7.58
Opening Twice-First Lap	4.41	−3.88	0.53	0.63	−6.40	−5.77	0.09	−8.85	−8.76
Opening Twice-Second lap	4.09	−4.93	−0.84	0.12	−4.70	−4.58	0.94	−8.81	−7.87

shut. This intermittent pattern of mass flow rate was observed in all three cases, namely when the door was opened once, and both laps of opening twice.Slight differences in air velocities right before door opening started (i.e., slightly different initial conditions) resulted in respective variations in the data, yet the overall pattern indicated that the effect of door opening could prevail these small differences in the flow. Furthermore, the absence of pressure differential facilitated the mixing of air both ways, though the total air exchange was nearly zero. These patterns changed dramatically by introducing positive pressure as the inward patterns followed by the door opening (2 − 3.5s) where suppressed by the positive pressure. In the presence of positive pressure, the 'balanced-mixing' across the door was changed to a 'directional pathway' from inside the room outward (i.e., negative mass flow rate values). Increasing pressure differential resulted in more pronounced directional pathways.

Areas under the curves shown in Fig. 8 indicate the total transport of mass (kg) across the door (Table 2). To put this in context, for $\Delta P = 20$Pa nearly 8.5 kg of air leaves room per door opening, which is equivalent to 7.5 m^3 of air when divided by the density of air (ρ = 1.125 kg/m^3). Literature shows that, on average, the operating room door is operated once every 3 min [19].Therefore, during 1 h of an average surgery 20 × 7.5 = 150 m^3 of air can leave the operating room. This is twice the volume of the test chamber, meaning that nearly 2 ACH of air escape the operating room and enter the adjacent corridor only due door openings. This number is equal to the ventilation rate required for patient corridors by Standards [47]. This air, if contaminated by the SARS-COVID-2 virus, can potentially spread into the adjacent corridors and jeopardize the safety of the medical personnel in the hallway.

3.3. Spatial distribution inside chamber

The data obtained from the peripheral ultrasound sensors indicated the behavior of the flow fields near the movement zone. The radial arrangement of the omnidirectional sensors provided the data to analyze spatial distribution of the wakes inside the chamber. The dissipation of velocity fields showed the impact of the door movement could last long after the door movement ceased.

Fig. 9 compare the velocity fields in the test chamber for standalone and consecutive door opening exercises, with the supply fan on working mode. For Test 3, at the initial periods of door opening, the isometric lines with higher velocity fields are concentrated in the movement zone and spread through the space with time. Two seconds after the door closure for Test 3, areas with significant velocity magnitude (> 0.1 m/s) were found up to 2 m from the tip of the door into the chamber. By 10 s after door closure, this field with velocities > 1 m/s penetrated 4.5 m inside the chamber.

During Test 5, when the supply fan was operating at the full capacity, the interaction between the external movement generated wakes and the high-velocity supply air resulted in a rise in the air speed, more than all the previous tests. Nearly everywhere in the chamber recorded velocity magnitudes greater than 1 m/s after 14 s of door closure, at which time, the maximum air speed recorded was 0.5 m/s. At second 23, 4 m inside the chamber, a maximum air speed 0.25 m/s were present. Starting from second 29, the fields started to shrink and by second 39, the maximum speed reduced to 0.14 m/s.

When the test setting involved movement of the door twice, for Tests 4 and 6, the magnitude of the velocity fields was found to be slightly increased compared to Tests 3 and 5, respectively. Data obtained during Test 4 showed that the wakes with velocity up to 0.12 m/s was present nearly 4 m inside the chamber. Even after 23 s since the first door opening began, > 1 m/s magnitude of velocity was measured at a distance of 4.75 m from the door.

During Test 6, by second 19, the maximum velocity magnitude inside the chamber was 0.6 m/s, owing to potential turbulence during consecutive door movements. From second 29, the supplied airflow started to push the wakes towards exit, but velocity magnitudes were present deep inside the chamber even at second 35.

It should be noted that the heatmaps presented in Fig. 9 were created considering zero slip condition at the walls. The known location and magnitudes of velocity, obtained from the radially arranged omnidirectional sensors, were interpolated to find the velocity values in the chamber that was discretized in a grid of size 110 x 109, where a square grid dimension was 5 cm.

4. Limitations

This paper aims to study the impacts of door opening in a positively pressurized chamber, which was hypothesized as an operating room where a COVID patient is to be receiving surgical intervention. Air mixing across a swing door and the resultant alterations in velocity field inside the chamber have been studied. It must be noted that the chamber used in this study was significantly smaller than a typical OR and the positive pressure magnitudes were higher than those recommended by Standards. Several previous studies have investigated the volumetric exchange between spaces separated by a door, ensuring differential pressures at the two compartments from numerical simulation approach [9,29] and experimental approach [23,30]. Experiments were repeated 60 times to ensure consistency and repeatability of the outcomes. Due to the large number of tests and restricted availability of the test facility, only two-scenarios of the door opening and closing cycles could be defined. At the time of these experiments, the ultrasound sensors were not fully commercialized and hence very few (17 out of 900 data points) unreasonable data logs (velocities greater than 2.5 m/s) were recorded, which were discarded during data analysis.

The possibility of a virus growth can be related to the humidity level in an indoor environment. In these sets of experiments, the relative humidity levels inside the test chamber was not measured, as the purpose of the study was to quantify the flow properties and understand their patterns. Future studies on the alterations of the relative humidity ratio could provide meaningful understanding of how SARS-CoV-2's viability alters with the flow properties.

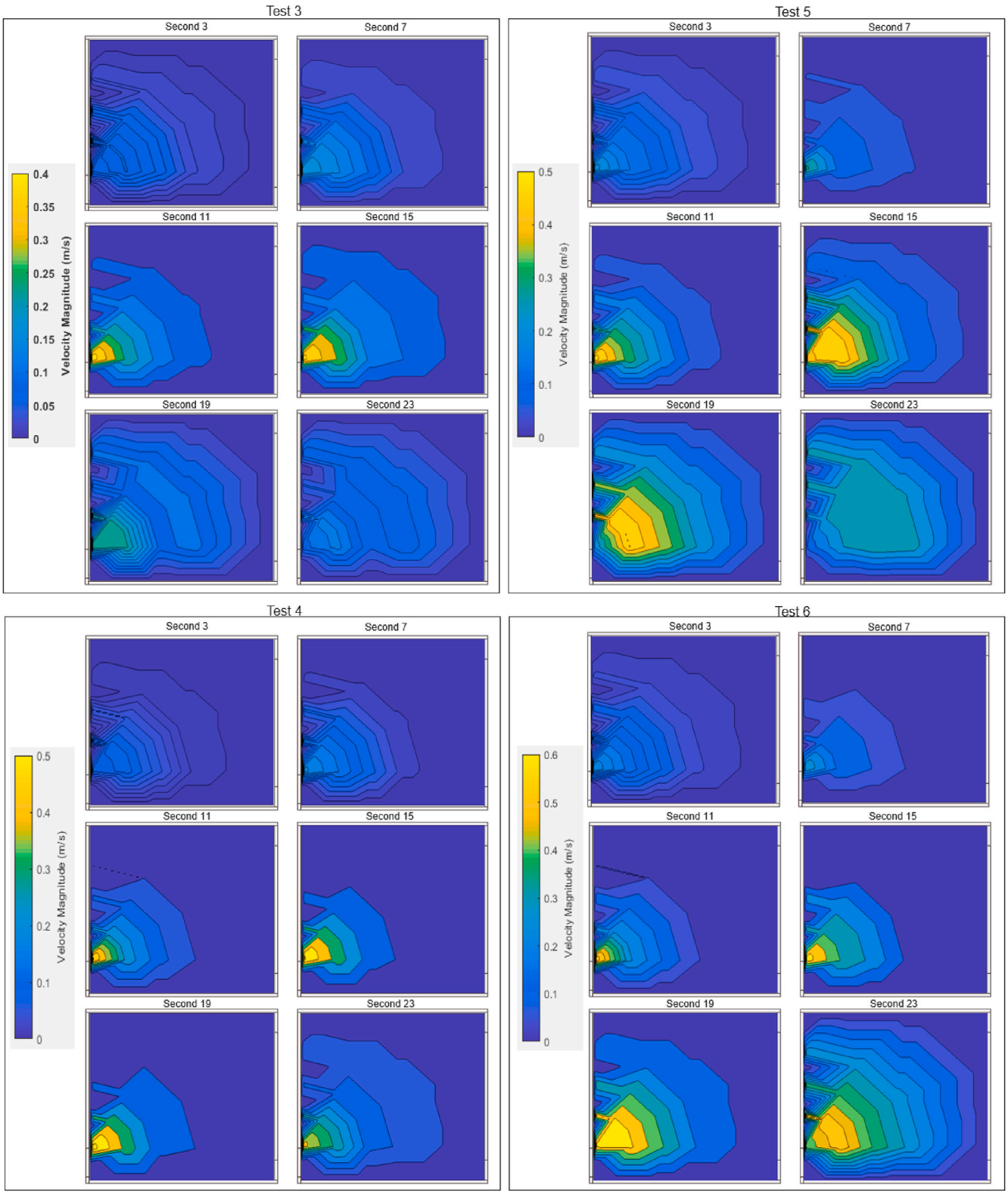

Fig. 9. Spatial distribution of velocity fields.

5. Conclusions

This experimental study was conducted in a sealed chamber with the capabilities of fresh air inlet at rates that generated sufficient positive pressure required for spaces like operating room. This study indicated that the transient change in the velocity field from door opening and closing were location specific – the points closest to the door tip responded to the changes quicker than those located farther, e.g. point 1 of the radial arrangements recorded changes quicker than point 4. Different points (*P*1, *P*2, and *P*3) in the vicinity of door swinging radius were also found to respond according to the door's position while opening or closing.

Emulating the opening and closing movement twice resulted in further increase of the flow velocity. During opening the door for the first time, disturbances are introduced to the quiescent air inside the chamber. While closing, more disturbances are introduced to an existing velocity field, that resulted in increased the velocity components. For Tests 3 and 5, i.e. one-cycle of door opening under ventilated condition, lower magnitudes of velocity were observed when compared to Test 1. The existing airflow suppressed the effect of door opening on the indoor flow fields. The second cycle of door movement interacted with the flow field under an existing motion exerted by the first cycle of door operation. Hence higher magnitude velocity components were recorded during Tests 2, 4, and 6, compared to Tests 1, 3, and 5.

The spatial distribution had provided insights about unwanted air mixing due to secondary velocity fields originating from door movement. The increase in air velocity inside the chamber was due to the wakes carried by the moving door in the background air. These wakes dissipate through the chamber and as they penetrate further into the chamber, the velocity field continued to decrease, due to the lost momentum during transfer between air molecules. But with supply fan working, the interaction between the primary flow field due to inlet air and the secondary flow fields due to door opening was higher and reached very far inside the chamber. Results from door opening twice indicated that with increased number of door operation, the secondary fields were stronger, and the increased interaction resulted in deeper penetration of wakes inside the chamber. These findings suggest that even with high quantity of supplied airflow, the door operation can disrupt the predominant flow pattern and the perturbation is capable to sustain long after the door was closed carrying high velocity air deep into the chamber. In a positively pressurized operating room with a contagious patient, this kind of air mixing is undesirable as the directional airflow from positive pressure differential is aimed to carry the contaminated air out of the facility.

A large proportion of this work was aimed at quantifying the air escape from the positively pressurized operating room due to door opening in order to gain insights about risks of air potentially contaminated with SARS-COVID-2 putting healthcare providers at risk. This study found that with inlet air flow rate of 190 cfm (90 L/s), 7.5 m^3 of air can leave for every time the swing door is operated. This translates to almost 2 ACH of air escaping during a typical surgical procedure, carrying contagions to the adjacent spaces. The future research should focus on utilizing the results of this study to imitate real-time operating procedure involving sporadic door opening, for further validation. Optimization of positive pressurization and exhaust locations for such sensitive procedures involving pathogens such as SARS-COV-2 is also one of the principal future research directions.

Declaration of competing interest

The authors declare that they have no known competing financial interests or personal relationships that could have appeared to influence the work reported in this paper.

Acknowledgement

We are thankful for the funds from US National Science Foundation under the Grant Number 2012827. The help and assistance from the faculty and staff at the Center for Built Environment in University of California, Berkeley are truly appreciated.

References

[1] Yan Bai, Lingsheng Yao, Wei Tao, Fei Tian, Dong-Yan Jin, Lijuan Chen, Meiyun Wang, Presumed asymptomatic carrier transmission of covid-19, Jama 323 (14) (2020) 1406–1407.
[2] Lidia Morawska, Junji Cao, Airborne transmission of sars-cov-2: the world should face the reality, Environ. Int. (2020) 105730.
[3] Rajat Mittal, Rui Ni, Jung-Hee Seo, The flow physics of covid-19, J. Fluid Mech. 894 (2020).
[4] Leonardo Setti, Fabrizio Passarini, Gianluigi De Gennaro, Pierluigi Barbieri, Maria Grazia Perrone, Massimo Borelli, Jolanda Palmisani, Alessia Di Gilio, Prisco Piscitelli, Alessandro Miani, Airborne Transmission Route of Covid-19: Why 2 Meters/6 Feet of Inter-personal Distance Could Not Be Enough, 2020.
[5] Xian Peng, Xin Xu, Yuqing Li, Lei Cheng, Xuedong Zhou, Biao Ren, Transmission routes of 2019-ncov and controls in dental practice, Int. J. Oral Sci. 12 (1) (2020) 1–6.
[6] Ehsan Mousavi, F. Betz, R. Lautz, Academic Research to Support Facility Guidelines Institute Ansi/ashrae/ashe Standard 170-2013, AHA Data Insight, 2019.
[7] Abigail Hathway, Ilias Papakonstantis, Adorkor Bruce-Konuah, Wernher Brevis, Experimental and modelling investigations of air exchange and infection transfer due to hinged-door motion in office and hospital settings, Int. J. Vent. 14 (2) (2015) 127–140.
[8] S.C. Hu, Y.Y. Wu, C.J. Liu, Measurements of air flow characteristics in a full-scale clean room, Build. Environ. 31 (2) (1996) 119–128.
[9] Ehsan S. Mousavi, Kevin R. Grosskopf, Airflow patterns due to door motion and pressurization in hospital isolation rooms, Sci. Technol. Built Environ. 22 (4) (2016) 379–384.
[10] Essam E. Khalil, Thermal management in healthcare facilities: computational approach, in: 47th AIAA Aerospace Sciences Meeting Including the New Horizons Forum and Aerospace Exposition, 2009, p. 1585.
[11] Ehsan S. Mousavi, Kevin R. Grosskopf, Secondary exposure risks to patients in an airborne isolation room: implications for anteroom design, Build. Environ. 104 (2016) 131–137.
[12] William Schaffner, An outbreak of airborne nosocomial varicella, Pediatrics 70 (1982) 550–556.
[13] Adele Josephson, Myles E. Gombert, Airborne transmission of nosocomial varicella from localized zoster, J. Infect. Dis. 158 (1) (1988) 238–241.
[14] Brian R. Edlin, Jerome I. Tokars, Michael H. Grieco, Jack T. Crawford, Julie Williams, Emelia M. Sordillo, Kenneth R. Ong, James O. Kilburn, Samuel W. Dooley, Kenneth G. Castro, et al., An outbreak of multidrug-resistant tuberculosis among hospitalized patients with the acquired immunodeficiency syndrome, N. Engl. J. Med. 326 (23) (1992) 1514–1521.
[15] Yiping Li, Gabriel M. Leung, J.W. Tang, Xiaozhan Yang, C.Y. Chao, John Zhang Lin, J.W. Lu, Per Væggemose Nielsen, J. Niu, H. Qian, et al., Role of ventilation in airborne transmission of infectious agents in the built environment-a multidisciplinary systematic review, Indoor Air 17 (1) (2007) 2–18.
[16] Clive B. Beggs, Kevin G. Kerr, J Noakes Catherine, E Abigail Hathway, P Andrew Sleigh, The ventilation of multiple-bed hospital wards: review and analysis, Am. J. Infect. Contr. 36 (4) (2008) 250–259.
[17] I. Eames, D. Shoaib, C.A. Klettner, V. Taban, Movement of airborne contaminants in a hospital isolation room, J. R. Soc. Interface 6 (suppl_6) (2009). S757–S766.
[18] Arup Bhattacharya, Andrew R. Metcalf, Ali Mohammadi Nafchi, Ehsan S. Mousavi, Particle dispersion in a cleanroom–effects of pressurization, door opening and traffic flow, Build. Res. Inf. (2020) 1–14.
[19] Ehsan S. Mousavi, Roxana Jafarifiroozabadi, Sara Bayramzadeh, Anjali Joseph, Dee San, An observational study of door motion in operating rooms, Build. Environ. 144 (2018) 502–507.
[20] Raymond J. Lynch, Michael J. Englesbe, Lisa Sturm, Amira Bitar, Karn Budhiraj, Sandeep Kolla, Yuliya Polyachenko, Mary G. Duck, Darrell A. Campbell Jr., Measurement of foot traffic in the operating room: implications for infection control, Am. J. Med. Qual. 24 (1) (2009) 45–52.
[21] Shital N. Parikh, Salih S. Grice, Beverly M. Schnell, Shelia R. Salisbury, Operating room traffic: is there any role of monitoring it? J. Pediatr. Orthoped. 30 (6) (2010) 617.
[22] Annette Erichsen Andersson, Ingrid Bergh, Jón Karlsson, Bengt I. Eriksson, Kerstin Nilsson, Traffic flow in the operating room: an explorative and descriptive study on air quality during orthopedic trauma implant surgery, Am. J. Infect. Contr. 40 (8) (2012) 750–755.
[23] Niklas Gustavsson, Dispersion of Small Particles into Operating Rooms Due to Door Openings, 2010.
[24] O. Ahmed, J.W. Mitchell, S.A. Klein, 3713 Dynamics of Laboratory Pressurization 99, ASHRAE Transactions-American Society of Heating Refrigerating Airconditioning Engin, 1993, pp. 223–229, 2.
[25] Dale T. Hitchings, Laboratory Space Pressurization Control Systems 36, ASHRAE Journal-American Society of Heating Refrigerating and Airconditioning Engineers, 1994, pp. 36–40, 2.
[26] D.E. Kiel, D.J. Wilson, Combining door swing pumping with density driven flow, Build. Eng. 95 (2) (1989) 590–599.
[27] Eric B. Smith, Ibrahim J. Raphael, Mitchell G. Maltenfort, Sittisak Honsawek, Kyle Dolan, Elizabeth A. Younkins, The effect of laminar air flow and door openings on operating room contamination, J. Arthroplasty 28 (9) (2013) 1482–1485.
[28] Carla Balocco, Giuseppe Petrone, Giuliano Cammarata, Assessing the effects of sliding doors on an operating theatre climate, in: Building Simulation, vol. 5, Springer, 2012, pp. 73–83.
[29] Sihwan Lee, Beungyong Park, Takashi Kurabuchi, Numerical evaluation of influence of door opening on interzonal air exchange, Build. Environ. 102 (2016) 230–242.
[30] Petri Kalliomäki, Pekka Saarinen, Julian W. Tang, Hannu Koskela, Airflow patterns through single hinged and sliding doors in hospital isolation rooms–effect of ventilation, flow differential and passage, Build. Environ. 107 (2016) 154–168.

[31] Bin Zhou, Lili Ding, Fei Li, Ke Xue, Peter V. Nielsen, Yang Xu, Influence of opening and closing process of sliding door on interface airflow characteristic in operating room, Build. Environ. 144 (2018) 459–473.
[32] Sagnik Mazumdar, Yanggao Yin, Arash Guity, Marmion Paul, Bob Gulick, Qingyan Chen, Impact of moving objects oncontaminant concentration distributions in an inpatient ward with displacement ventilation, HVAC R Res. 16 (5) (2010) 545–563.
[33] J.M. Villafruela, J.F. San José, F. Castro, Andrés Zarzuelo, Airflow patterns through a sliding door during opening and foot traffic in operating rooms, Build. Environ. 109 (2016) 190–198.
[34] Zhang Lin, T.T. Chow, C.F. Tsang, Effect of door opening on the performance of displacement ventilation in a typical office building, Build. Environ. 42 (3) (2007) 1335–1347.
[35] Ilias G. Papakonstantis, Elizabeth Abigail Hathway, Wernher Brevis, An experimental study of the flow induced by the motion of a hinged door separating two rooms, Build. Environ. 131 (2018) 220–230.
[36] Arup Bhattacharya, Ehsan Mousavi, The effect of boundary conditions on transient airflow patterns: a numerical investigation of door operation, Build. Eng. 126 (1) (2020).
[37] Fred Bauman, Edward A. Arens, S. Tanabe, H. Zhang, A. Baharlo, Testing and Optimizing the Performance of a Floor-Based Task Conditioning System, 1995.
[38] Nan Li, Qiong Chen, Study on dynamic thermal performance and optimization of hybrid systems with capillary mat cooling and displacement ventilation, Int. J. Refrig. 110 (2020) 196–207.
[39] Xiuyuan Du, Baizhan Li, Hong Liu, Yuxin Wu, Tengfei Cheng, The appropriate airflow rate for a nozzle in commercial aircraft cabins based on thermal comfort experiments, Build. Environ. 112 (2017) 132–143.
[40] Yuxin Wu, Hong Liu, Baizhan Li, Yong Cheng, Diyi Tan, Zhaosong Fang, Thermal comfort criteria for personal air supply in aircraft cabins in winter, Build. Environ. 125 (2017) 373–382.
[41] Marek Jaszczur, Pawel Madejski, Slawosz Kleszcz, Marcin Zych, Patryk Palej, Numerical and experimental analysis of the air stream generated by square ceiling diffusers, in: E3S Web of Conferences, vol. 128, EDP Sciences, 2019, 08003.
[42] Marek Borowski, Marek Jaszczur, Daniel Satoła, Michał Karch, Air flow characteristics of a room with air vortex diffuser, in: MATEC Web of Conferences, vol. 240, EDP Sciences, 2018, 02002.
[43] Ali Ghahramani, Megan Zhu, Richard Przybyla, Michael Andersen, Syung Min, Hui Zhang, Therese Peffer, Edward Arens, An inexpensive low-power ultrasonic 3-dimensional air velocity sensor, in: 2019 IEEE SENSORS, IEEE, 2019, pp. 1–4.
[44] Ali Ghahramani, Megan Zhu, Richard J. Przybyla, Michael P. Andersen, Parson J. Galicia, Therese E. Peffer, Hui Zhang, Edward Arens, Measuring air speed with a low-power mems ultrasonic anemometer via adaptive phase tracking, IEEE Sensor. J. 19 (18) (2019) 8136–8145.
[45] Edward Arens, Ghahramani Ali, Richard Przybyla, Michael Andersen, Syung Min, Therese Peffer, Paul Raftery, Megan Zhu, Vy Luu, Hui Zhang, Measuring 3d indoor air velocity via an inexpensive low-power ultrasonic anemometer, Energy Build. 211 (2020) 109805.
[46] Arup Bhattacharya, Jovan Pantelic, Ghahramani Ali, Ehsan S. Mousavi, Three-dimensional analysis of the effect of human movement on indoor airflow patterns, Indoor Air 31 (2) (2021) 587–601.
[47] ASHRAE, Standard 170–2013: Ventilation of Healthcare Facilities. Ventilation of Health Care Facilities, ASHRAE, 2013.